

GenAgent: Scaling Text-to-Image Generation via Agentic Multimodal Reasoning

Kaixun Jiang¹, Yuzheng Wang^{2†}, Junjie Zhou³, Pandeng Li^{2,4},
Zhihang Liu⁴, Chen-Wei Xie², Zhaoyu Chen¹, Yun Zheng², Wenqiang Zhang¹

¹Fudan University ²Tongyi Lab ³Nanjing University ⁴University of Science and Technology of China

Abstract

We introduce GenAgent, unifying visual understanding and generation through an agentic multimodal model. Unlike unified models that face expensive training costs and understanding-generation trade-offs, GenAgent decouples these capabilities through an agentic framework: understanding is handled by the multimodal model itself, while generation is achieved by treating image generation models as invokable tools. Crucially, unlike existing modular systems constrained by static pipelines, this design enables autonomous multi-turn interactions where the agent generates multimodal chains-of-thought encompassing reasoning, tool invocation, judgment, and reflection to iteratively refine outputs. We employ a two-stage training strategy: first, cold-start with supervised fine-tuning on high-quality tool invocation and reflection data to bootstrap agent behaviors; second, end-to-end agentic reinforcement learning combining pointwise rewards (final image quality) and pairwise rewards (reflection accuracy), with trajectory resampling for enhanced multi-turn exploration. GenAgent significantly boosts base generator(FLUX.1-dev) performance on GenEval++ (+23.6%) and WISE (+14%). Beyond performance gains, our framework demonstrates three key properties: 1) cross-tool generalization to generators with varying capabilities, 2) test-time scaling with consistent improvements across interaction rounds, and 3) task-adaptive reasoning that automatically adjusts to different tasks. Our code will be available at [this url](https://this.url).

1. Introduction

Understanding and generation represent the two foundational pillars of multimodal intelligence [6, 20]. A growing body of research indicates [2, 7, 30, 31] that a tight integration of these functions can yield significant gains in complex generative tasks. Current approaches can be broadly categorized into two paradigms: integrated end-to-end models, modular and decoupled systems. The in-

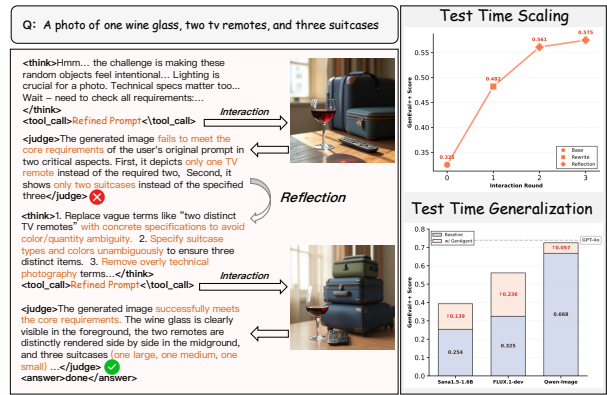


Figure 1. The left shows the illustration of GenAgent’s iterative interaction with image generation tools. The right presents the performance scaling of our GenAgent across interaction rounds (top) and generalization to different image generation tools (bottom).

tegrated approach involves either incorporating more powerful understanding modules directly into generative models [2, 31] or developing unified architectures [3, 4, 7, 10] capable of processing interleaved image-text inputs to facilitate complex reasoning chains [14, 15, 25]. Nevertheless, such tightly-coupled designs are often constrained by performance trade-offs [19] and require extensive computational resources for training [7].

Conversely, the modular paradigm provides enhanced flexibility and extensibility by separating reasoning from generation. In this configuration, a dedicated reasoning model handles the semantic understanding, while a generative model is tasked exclusively with image rendering. Re-Prompt [32] and PromptEnhancer [28], focus on single-turn prompt refinement. More recent works [29, 40] employ pre-defined, open-loop static workflows, assigning fixed roles to a cascade of models. The performance of these systems is inherently limited by their inability to make autonomous decisions or adapt dynamically.

To address this limitation, we introduce GenAgent, an agentic framework that unifies visual understanding and generation through iterative tool interaction. GenAgent is architected around an agentic multimodal model that exe-

[†]indicates project leader.

cutes autonomous multi-turn reasoning and generation: it formulates action plans, invokes external image generators as tools, evaluates their outputs, and engages in reflective reasoning to determine whether and how to proceed. Throughout this process, the agent generates multimodal chains-of-thought encompassing reasoning, tool invocation, judgment, and reflection. This design preserves the flexibility and interpretability of the modular paradigm while enabling deep, adaptive integration of reasoning and generation capabilities. Figure 1 (left) illustrates a representative two-turn interaction.

We propose a novel two-stage training framework for GenAgent. In the first stage, we construct high-quality SFT data through hint-guided distillation. We provide the advanced model with explicit criteria and reference images to ensure it generates accurate and well-reasoned tool invocation and reflection trajectories for cold-starting multi-turn agent behaviors. In the subsequent agentic reinforcement learning (RL) stage, we introduce a hybrid reward mechanism that combines pointwise outcome rewards—which assess final image quality—with pairwise process rewards that incentivize accurate reflections across consecutive rounds. We further employ a resampling strategy on interaction rounds that oversamples diverse trajectories and uniformly resamples across different rounds to expand the exploration space. Through this paradigm, GenAgent learns autonomous multi-round tool invocation and adaptive decision-making.

We evaluate GenAgent on challenging benchmarks. Without modifying the underlying image generators, GenAgent significantly boosts the base generator (FLUX.1-dev[16]) performance by +23.6% on GenEval++ and +14% on WISE. When equipped with stronger generation tools like Qwen-Image [31], our framework approaches the performance of the closed-source GPT-4o [20]. Our analysis reveals three key emergent properties: 1) **Cross-tool generalization**: GenAgent trained through interactions with FLUX.1-dev robustly transfers to other tools with varying capabilities (Figure 1, bottom right); 2) **Test-time scaling**: performance improves consistently across interaction rounds through multi-turn refinement (Figure 1, top right); and 3) **Task-adaptive reasoning**: distinct reasoning patterns emerge automatically for different task requirements (Section 4.5). We hope our agentic framework offers a promising path toward advancing unified visual understanding and generation. Our contributions are as follows:

- We introduce GenAgent, an agentic multimodal model that decouples understanding and generation by treating image generators as invokable tools, enabling autonomous reasoning and interaction through multimodal chains-of-thought.
- We propose a two-stage training framework with cold-start SFT on curated tool-invocation and reflection trajec-

tories and agentic RL using hybrid outcome-process rewards and resampling on interaction rounds.

- We demonstrate substantial gains on three challenging generation tasks, achieving competitive performance with both open-source and closed-source unified models while uncovering emergent properties including cross-tool generalization, test-time scaling, and adaptive reasoning.

2. Related Work

Understanding for generation. Current approaches to enhancing understanding for controllable generation fall into two paradigms: integrated end-to-end models and modular decoupled systems. The integrated paradigm either incorporates stronger understanding modules into generative models [2, 27, 31] or builds unified architectures [4, 7, 10, 30, 34] for complex multimodal reasoning. However, this design faces understanding-generation trade-offs and demands substantial training resources. The modular paradigm separates reasoning and generation, offering greater flexibility and lower costs. While early efforts like RePrompt [32] employed simple prompt optimization, recent workflows [29, 40] incorporate multiple models in pre-defined pipelines with fixed sequences, limiting adaptability to intermediate results. GenAgent addresses these limitations by elevating the modular paradigm from static workflow to dynamic agent. Through an agentic multimodal model-driven closed-loop mechanism, GenAgent autonomously plans, invokes tools, evaluates outputs, and iteratively refines strategies, substantially expanding the performance ceiling of modular approaches.

Agentic multimodal reasoning. Agentic reasoning has emerged as a powerful paradigm for complex multimodal tasks. In visual understanding, the “thinking with image” concept, pioneered by OpenAI’s O3[21], empowers models with external tools to refine reasoning—evolving from single-function tools like [39] to writing Python code for diverse image manipulations like [37]. In contrast, multimodal generation has predominantly relied on unified models [8, 14, 15, 18, 25], which integrate reasoning and generation within a single architecture. However, this tightly-coupled design limits flexibility and scalability: enhancing one capability (e.g., generation quality) requires costly retraining of the entire model. Our work addresses this limitation by pioneering a decoupled agentic framework for generation. An agentic multimodal model serves as the reasoning agent while image generators function as callable external tools. This design enables significant advantages: generative performance can be directly improved by upgrading tool components without retraining the core agentic structure, ensuring superior flexibility and scalability.

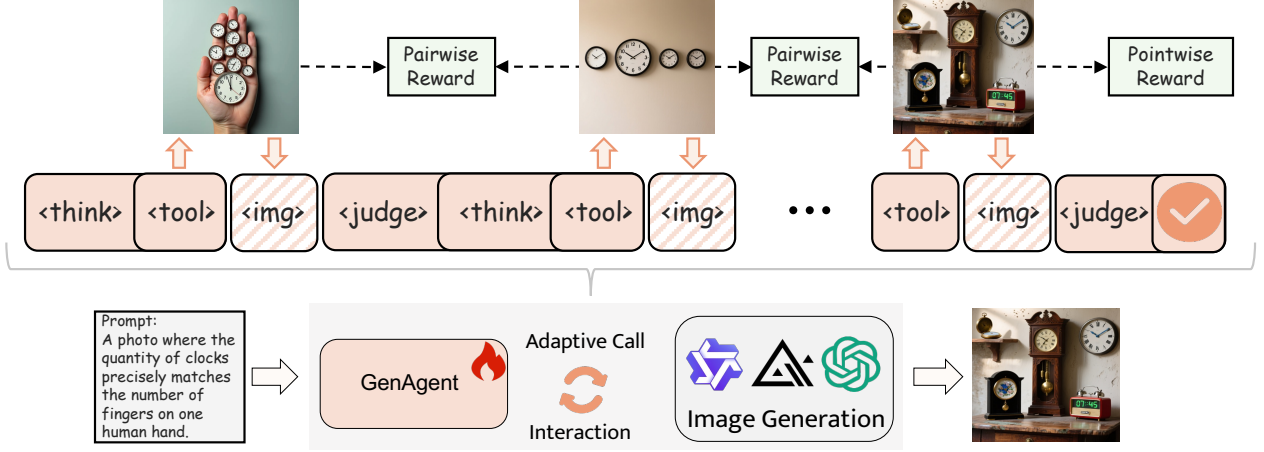


Figure 2. Overview of GenAgent. Upon receiving user input, GenAgent executes a multi-modal reasoning trace that encompasses iterative reasoning and image generation through dynamic interaction with image generation tools. During the rollout of agentic reinforcement learning, we compute pointwise rewards from the final image and pairwise rewards based on consecutive image pairs throughout trace.

3. Method

3.1. Overall Pipeline

Overall. Unlike existing single-step rewrite frameworks [28, 32] and multi-model workflows [29, 40], GenAgent is an agentic framework for multimodal generation. As shown in Figure 2, it comprises two core components: a **multimodal model** π_θ and an **interactive image generation tool**. Within each inference trajectory, GenAgent iteratively invokes the generation tool, orchestrating cycles of **thinking, generation, judgment, and reflection** until the output satisfies user requirements or reaches maximum interaction rounds n_{\max} . Figure 2 illustrates the pipeline of our method.

Initial Phase. GenAgent first receives user query q and reasons about the intent to produce an refined prompt P_1 in tool-callable format:

$$T_1, P_1 = \pi_\theta(q), \quad (1)$$

where T_1 denotes the reasoning trace. The prompt P_1 is passed to the image generation tool to produce $I_1 = \text{ImageGen}(P_1)$.

Judgment and Reflection. Then, GenAgent evaluates I_1 against user requirements:

$$\pi_\theta(q, T_1, P_1, I_1) = \begin{cases} (J_1, a), & \text{if } I_1 \text{ satisfies } q \\ (J_1, T_2, P_2), & \text{otherwise} \end{cases} \quad (2)$$

where J_1 is the judgment trace and a denotes termination. If the result is satisfactory, the system outputs a . Otherwise, J_1 identifies deficiencies and T_2, P_2 guide the next iteration. This process continues until satisfaction or maximum rounds n_{\max} is reached. A complete multimodal reasoning

trajectory (corresponding to the upper part of Figure 2) is:

$$o = \{q, T_1, P_1, I_1, J_1, \dots, T_n, P_n, I_n, J_n, a\}, \quad (3)$$

where $n \leq n_{\max}$ denotes the actual number of interaction rounds. o captures the complete multimodal chains-of-thought and self-correction capability. The final generated image I_n serves as the output.

3.2. Supervised Fine-Tuning

Table 1. Diagnostic analysis of Base and SFT models on GenEval++ [35]. Error Rate represents the tool invocation failure rate, Word Diffs denotes the word count difference between the final prompt and user input, and improvement indicates the performance gain attributed to reflection.

Stage	Error Rate(%)	Word Diffs <= 5(%)	Improvement(%)
Base	13.36	49.28	0.36
+SFT	0.35	0.00	6.07

We first investigate whether multimodal models possess sufficient zero-shot capability for this task. Specifically, we evaluate Qwen2.5-VL-7B [1] and identify three critical limitations as shown in Table 1: 1) Unreliable tool invocation; 2) Ineffective reflection; 3) Poor refinement. These limitations indicate that direct RL would be inefficient: invocation errors prevent effective interaction with generators, weak reflection hinders learning from feedback, and poor refinement leads to limited RL exploration. Therefore, a cold-start phase is essential.

3.2.1. Data Construction Pipeline

Figure 3 illustrates the complete trajectory synthesis pipeline for cold-start training data. All system prompts,

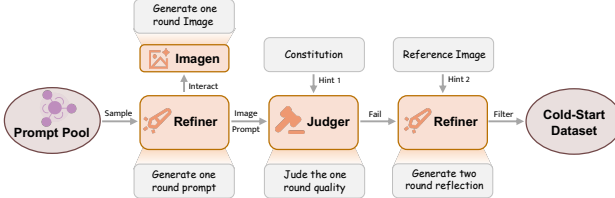


Figure 3. SFT data construction pipeline.

data sources, and distributions are provided in the supplementary materials (Supp).

Prompt Pool. To enable the model to effectively learn tool invocation and reflection capabilities, we carefully curate sufficiently challenging training data. Specifically, we first collect open-source data, then construct synthetic data requiring complex reasoning to match the difficulty of multi-turn tool invocation (detailed pipeline in supplementary materials; Figure 2 shows a synthetic case with original prompt ‘a photo of five clocks’). We filter these through FLUX.1-dev [16] with 3-pass generation, retaining only samples where all attempts fail.

One-round Trajectory Synthesis. The first round aims to teach the model the format for reasoning and invoking the image generation tool. We employ Qwen3-VL-235B-A22B-Thinking [22] as the teacher model for distillation to obtain the thinking process and the refined prompt P_1 . After filtering out format-incorrect samples, we feed all refined prompts to the FLUX.1-dev to produce the corresponding images.

Judging Synthesis. Inspired by [12], we provide explicit rules for the model to judge whether the generated image satisfies the prompt requirements and output the reasoning behind the judgment. This allows the model to implicitly learn these evaluation criteria during training, even though they are not explicitly provided during inference. We retain samples judged as successful, while unsuccessful ones proceed to the two-round reflection.

Reflection Synthesis. We prompt the model to refine the one round P_1 based on the user’s original input q and previous evaluation results J_1 . To ensure high-quality reflection, we implement two key improvements: First, we upgrade to the more capable Gemini 2.5 Pro [6] as the teacher model. Second, since the seed prompt pool is derived from SFT data, all examples have corresponding reference images. We leverage these reference images as additional guidance for the second-round refinement. We filter out trajectories that explicitly reference the hint image in their prompts, then generate new images using the refined second-round prompts. Through pairwise comparison, we eliminate cases where the second round produces inferior results compared to the first. Finally, we apply pointwise evaluation to assess whether the second-round images satisfy user requirements,

retaining only those samples that meet quality standards.

Data Sampling Strategy. Through the above pipeline, we construct two-round training data with tool invocation and reflection. We further filter out samples with logical inconsistencies in the trajectories. Finally, we perform balanced sampling based on data type and whether the second round terminates, ultimately obtaining 32K high-quality cold-start data samples. Notably, we intentionally avoid having all samples end with a to ensure the model is not limited to single-round reflection, thereby preserving exploration space for subsequent reinforcement learning.

3.2.2. Training Strategy

To mitigate hallucination and leverage high-quality trajectories, we mask environment feedback tokens and compute loss only on model responses. Figure 3 shows that SFT successfully addresses the base model’s limitations: (1) tool invocation errors decrease substantially, (2) refined prompts become longer and more detailed (see Supplementary Material), and (3) reflection quality improves markedly.

3.3. Agentic Reinforcement Learning

After cold-start training, GenAgent has acquired basic tool-calling capabilities. However, SFT relies on fixed round trajectories for imitation learning, making it difficult to generalize to complex scenarios requiring more rounds or to learn when to stop reflection. Therefore, we introduce reinforcement learning to train the model’s dynamic decision-making abilities. We adopt GRPO [13]. For each query q , GRPO samples a group of trajectories $\{o_1, \dots, o_G\}$ from policy π_θ and optimizes via:

$$\mathcal{J}(\theta) = \frac{1}{G} \sum_{i=1}^G \frac{1}{|o_i|} \sum_{t=1}^{|o_i|} \left\{ \min \left[\text{clip}(\sigma_{i,t}, 1 - \epsilon, 1 + \epsilon) A_i, \sigma_{i,t} A_i \right] \right\}, \quad (4)$$

where $\sigma_{i,t} = \frac{\pi_\theta(o_{i,t}|q, o_{i,<t})}{\pi_{\theta_{\text{old}}}(o_{i,t}|q, o_{i,<t})}$ denotes the likelihood ratio between the updated and old policies at step t . ϵ is a hyper-parameter. In agentic RL [39], we compute the loss only on the output tokens generated by π_θ , while masking environment observations (i.e., the generated images I in trajectory o). The group-normalized advantage, denoted as A_i , is calculated by the reward r_i :

$$A_i = \frac{r_i - \text{mean}(\{r_i\}_{i=1}^G)}{\text{std}(\{r_i\}_{i=1}^G)}. \quad (5)$$

Existing RL methods [13, 36] for reasoning tasks often use rule-based outcome rewards to avoid reward hacking. However, Our task face two challenges: 1) image quality is difficult to quantify; 2) outcome rewards are too coarse-grained, failing to distinguish the quality of effective reflection trajectories. We propose a hybrid reward mechanism combining pointwise and pairwise rewards.

Pointwise Reward. We employ an advanced MLLM as a Generative Reward Model [17] to verify whether the final

generated image satisfies all specified conditions. To ensure evaluation reliability, we implement three key strategies: 1) We prompt the MLLM to first generate step-by-step reasoning before making the final judgment. 2) We provide detailed evaluation criteria along with condition-specific hints for each sample to guide accurate assessment. 3) We enforce strict rewards where the agent receives a reward only when all conditions are satisfied; otherwise, the reward is 0.

Pairwise Reward. To encourage effective reflection while preventing reward hacking [9], we introduce process rewards based on a key insight: genuine reflection should yield consistent quality improvement across the entire trajectory. We grant rewards only when the MLLM judges that all subsequent images are superior to their predecessors:

$$r_{\text{pair}} = \begin{cases} 0.3 & \text{if } M_{\text{judge}}(I_k, I_{k+1}) = I_{k+1}, \forall k \in [1, n-1], \\ 0 & \text{otherwise,} \end{cases} \quad (6)$$

where $M_{\text{judge}}(I_k, I_{k+1})$ returns the better image between consecutive pairs. To avoid positional bias, the positions are randomly shuffled. The final reward is:

$$r = r_{\text{point}} + r_{\text{format}} + \lambda \cdot r_{\text{pair}}, \quad (7)$$

where $r_{\text{point}} \in \{0, 0.7\}$, $r_{\text{format}} \in \{0, -0.2\}$, $\lambda = 0.5$ if $r_{\text{point}} = 0$ else $\lambda = 1$.

Resampling on Interaction Rounds. Motivated by [23], considering that trajectories with different numbers of interaction turns correspond to distinct reasoning traces (e.g., single-turn interactions primarily focus on rewriting and judging, while multi-turn interactions involve reflection), we adopt a resampling strategy based on interaction turns. Specifically, during the rollout phase, we oversample G' trajectories ($G' > G$), and then uniformly resample according to the number of interaction turns. This approach enables the model to observe more diverse trajectories and expands the exploration space.

4. Experiments

4.1. Implementation Details

We initialize our approach using Qwen2.5-VL-7B [1] as the base model and perform supervised fine-tuning via the LLaMAFactory [38], employing a batch size of 256 and a learning rate of 1×10^{-5} . The model undergoes optimization across 3 epochs utilizing the AdamW optimizer. In the subsequent reinforcement learning phase, we implement an enhanced GRPO with a batch size of 240. For each prompt, we generate $G' = 12$ rollouts, which are then downsampled to $G = 8$ samples. The KL divergence coefficient is set to 0.0 [36], the maximum response length is capped at 16,384 tokens, and a learning rate of 1×10^{-6} is adopted. We leverage the 8-step distilled version of FLUX.1-dev [16] as our

interactive image generation tool, maximum number of interactions $n_{\text{max}} = 3$; all subsequent references to FLUX.1-dev correspond to this specific version. Through efficient and robust server deployment, we substantially improve rollout efficiency. We employ Qwen3-VL-30B-A3B [22] as the generative reward model. The complete training framework is implemented using verl [24].

4.2. Benchmarks

We select three challenging benchmarks to evaluate our method across multiple dimensions: (1) **Instruction-following:** GenEval++ [35], a more accurate and challenging benchmark for evaluating instruction fidelity in image generation, featuring richer semantics and more diverse compositions than the original GenEval [11]. (2) **Knowledge-grounded reasoning:** WISE [19], which comprehensively assesses complex semantic understanding and world-knowledge integration in text-to-image generation. (3) **Creative generation:** Imagine [35], designed to evaluate surreal and imaginative image generation capabilities by testing the model’s ability to augment common objects with fantastical elements while preserving their core identity—often requiring outputs that contradict factual reality.

4.3. Performance Comparison

We selected representative baselines spanning different paradigms: 1) Diffusion models: Qwen-Image [31] and FLUX.1.dev [16]; 2) Unified architectures: the autoregressive Janus-Pro-7B [4], reasoning-focused T2I-R1 [15], hybrid-architecture Bagel [7], and closed-source GPT-4o [20]; 3) Decoupled approaches: PromptEnhancer (7B version) [28] and ReflectionFlow [40]. These methods and GenAgent use FLUX.1.dev as the default image generation tool. For fair comparison and efficiency, we report results with $n_{\text{max}} = 2$ for all multi-turn baselines and our method. We report our GenAgent across multiple variants: without tool invocation, degenerating to a single-pass rewrite model (w/o tool), with SFT (+SFT), with RL (+RL), and with a stronger tool (w/ Qwen-Image).

Diffusion Models. GenAgent substantially enhances diffusion model performance across all benchmarks. When FLUX.1-dev is equipped with our GenAgent framework, it achieves substantial improvements: +0.14 on WISE (0.69 vs. 0.55), +0.236 on GenEval++ (0.561 vs. 0.325), and +0.753 on ImagineBench (6.825 vs. 6.072). Notably, despite RL training with FLUX, GenAgent generalizes effectively to the stronger Qwen-Image generator, achieving 0.72, 0.725, and 7.803—new state-of-the-art results among open-source methods. This demonstrates weak-to-strong scalability at the tool level, analyzed in detail in Section 4.4.

Unified Architectures. On knowledge-grounded reasoning (WISE), GenAgent w/ FLUX.1-dev achieves 0.69, matching the specialized Bagel w/ Self-CoT (0.70), while GenA-

Table 2. Performance Comparison on GenEval++. **bold** indicates the best result.

Type	Method	Color	Count	Color/Count	Color/Pos	Pos/Count	Pos/Size	Multi-Count	Overall
Diffusion	FLUX.1-dev	0.400	0.600	0.250	0.250	0.075	0.400	0.300	0.325
	Qwen-Image	0.875	0.725	0.725	0.600	0.475	0.725	0.550	0.668
Unified	GPT4o	0.900	0.675	0.725	0.625	0.600	0.800	0.850	0.739
	Janus Pro 7B	0.450	0.300	0.125	0.300	0.075	0.350	0.125	0.246
	T2I-R1	0.675	0.325	0.200	0.350	0.075	0.250	0.300	0.311
Decoupled	Bagel	0.325	0.600	0.250	0.325	0.250	0.475	0.375	0.371
	PromptEnhancer	0.500	0.625	0.225	0.375	0.125	0.450	0.375	0.382
	ReflectionFLow	0.400	0.625	0.275	0.275	0.200	0.425	0.325	0.361
GenAgent (Ours)	Ours w/o tool	0.650	0.575	0.350	0.450	0.350	0.600	0.400	0.482
	Base	0.300	0.600	0.325	0.300	0.325	0.300	0.350	0.357
	+SFT	0.500	0.550	0.550	0.525	0.250	0.600	0.575	0.507
	+RL	0.750	0.675	0.375	0.525	0.450	0.625	0.525	0.561
	w/ Qwen-Image	0.775	0.775	0.650	0.800	0.600	0.725	0.750	0.725

Table 3. Performance Comparison on WISE. **bold** indicates the best result.

Type	Method	Cultural	Time	Space	Biology	Physics	Chemistry	Overall
Diffusion	FLUX.1-dev	0.56	0.57	0.67	0.45	0.54	0.41	0.55
	Qwen-Image	0.62	0.63	0.77	0.57	0.75	0.40	0.62
Unified	GPT4o	0.81	0.71	0.89	0.83	0.79	0.74	0.80
	Janus Pro 7B	0.30	0.37	0.49	0.36	0.42	0.26	0.35
	T2I-R1	0.56	0.55	0.63	0.54	0.55	0.30	0.54
	Bagel	0.44	0.55	0.68	0.44	0.60	0.39	0.52
Decoupled	Bagel w/ Self-CoT	0.76	0.69	0.75	0.65	0.75	0.58	0.70
	PromptEnhancer	0.54	0.60	0.69	0.46	0.62	0.39	0.56
	Ours w/o tool	0.75	0.66	0.72	0.55	0.60	0.49	0.67
GenAgent (Ours)	Base	0.70	0.63	0.68	0.53	0.61	0.41	0.63
	+SFT	0.68	0.61	0.68	0.60	0.65	0.47	0.64
	+RL	0.75	0.69	0.72	0.61	0.65	0.50	0.69
	w/ Qwen-Image	0.78	0.67	0.78	0.72	0.71	0.55	0.72

gent w/ Qwen-Image reaches 0.72, surpassing all open-source unified models and approaching GPT-4o (0.80). For instruction-following (GenEval++), GenAgent with Qwen-Image (0.725) nearly matches GPT-4o (0.739) and significantly outperforms other open-source alternatives. On creative generation (Imagine), GenAgent with Qwen-Image (7.794) substantially narrows the gap with GPT-4o (8.560) while establishing a clear lead over the second-best T2I-R1 (6.780). These results demonstrate that our agentic framework achieves superior generalization and scalability compared to unified architectures, while maintaining competitive performance on complex generative tasks.

Decoupled Methods. GenAgent substantially outperforms existing decoupled approaches. Single-rewrite PromptEnhancer achieves only marginal gains over vanilla FLUX: 0.56 on WISE (+0.01), 0.382 on GenEval++ (+0.057), and 6.281 on Imagine (+0.209). Workflow-based ReflectionFlow reaches 0.361 on GenEval++, significantly below GenAgent’s 0.561 (+0.2). Notably, even without the agen-

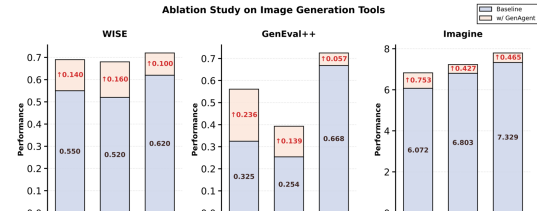


Figure 4. Ablation study on image generation tools.

tic framework, using only one rewriting (Ours w/o tool), our method outperforms PromptEnhancer across all benchmarks. These results indicate that existing decoupled methods underutilize multimodal model reasoning capabilities. In contrast, GenAgent’s end-to-end agentic loop with iterative judgment and reflection unlocks significant potential.

4.4. Ablation Study

Training Stage. We conduct ablation studies to assess the contribution of each training stage (Table 5). The initial

Table 4. Performance Comparison on Imagine. **bold** indicates the best result.

Type	Method	Attribute Shift	Spatiotemporal	Hybridization	Multi-Object	Overall
Diffusion	FLUX.1-dev	5.298	6.350	7.053	5.973	6.072
	Qwen-Image	6.771	7.193	8.130	7.500	7.329
Unified	GPT4o	8.540	9.180	8.570	7.980	8.560
	Janus Pro 7B	5.300	7.280	6.730	6.040	6.220
	T2I-R1	5.850	7.700	7.360	6.680	6.780
	Bagel	5.370	6.930	6.500	6.410	6.200
Decoupled	PromptEnhancer	5.489	6.213	7.327	6.493	6.281
	Ours w/o tool	5.829	6.827	7.130	6.137	6.408
GenAgent (Ours)	Base	5.467	6.590	7.287	6.083	6.258
	+SFT	6.282	7.033	7.480	6.527	6.770
	+RL	6.293	7.067	7.543	6.663	6.825
	w/ Qwen-Image	7.613	7.547	8.343	7.763	7.794

Table 5. Ablation study on training stages. Subscripts represent the gains attributed to reflection.

Stage	WISE	GenEval++	Imagine
Base	0.63	0.357	6.258
SFT	0.64	0.507	6.770
RL w/o r_{pair}	0.68 _{+0.01}	0.543 _{+0.068}	6.814 _{+0.168}
RL(Ours)	0.69_{+0.02}	0.561_{+0.079}	6.825_{+0.417}

Supervised Fine-Tuning (SFT) stage improves instruction-following (GenEval++) and creativity metrics (Imagine) but yields limited gains on the knowledge-intensive WISE benchmark. This is because SFT primarily focuses on learning “how to respond” rather than exploring to activate the model’s intrinsic reasoning capabilities. The subsequent RL phase (RL w/o r_{pair}) improves performance across all metrics, demonstrating that RL-based exploration can effectively elicit the model’s latent reasoning capabilities. Most critically, the full model incorporating our reflection reward, RL(Ours), achieves the strongest performance overall. Compared to its counterpart without the pairwise reward, our method delivers substantially greater reflection-induced improvements, which translate directly into superior downstream performance. This validates the effectiveness of our r_{pair} design in amplifying the value of reflection within the agentic framework.

Image Generation Tools. As illustrated in Figure 4, although our GenAgent uses FLUX.1-dev as the image generation tool during reinforcement learning, it demonstrates exceptional cross-tool generalization and scalability. When replacing the tool with the small Sana1.5-1.6B model [33], GenAgent still achieves significant improvements across all three benchmarks, demonstrating strong backward compatibility. More encouragingly, when employing the more powerful Qwen-Image, GenAgent further enhances its overall performance. This phenomenon indicates that our method

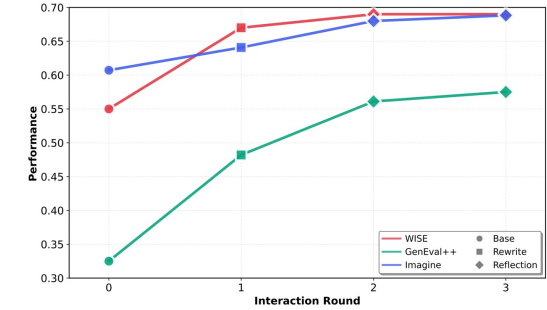


Figure 5. Ablation on interaction rounds, with normalized scores.

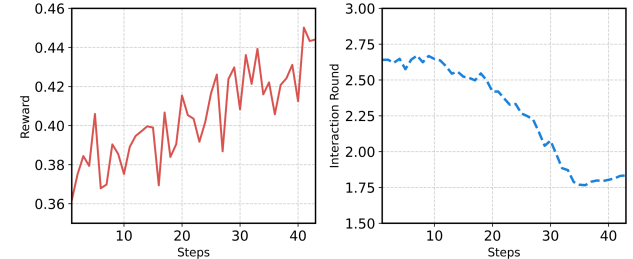


Figure 6. Training dynamics on reward and interaction rounds.

can scale with the capability improvements of underlying image generation tools, fully unleashing the potential of advanced generative models.

Interaction Rounds. Figure 5 illustrates the impact of different interaction rounds with the image generation tool on performance. The first interaction demonstrates GenAgent’s rewriting capability, with all benchmarks exhibiting significant performance improvements, indicating that initial prompt rewriting effectively comprehends and refines users’ original prompts. The second interaction round showcases the effectiveness of the first reflection, with all three tasks showing varying degrees of performance gains, confirming that the reflection mechanism successfully opti-

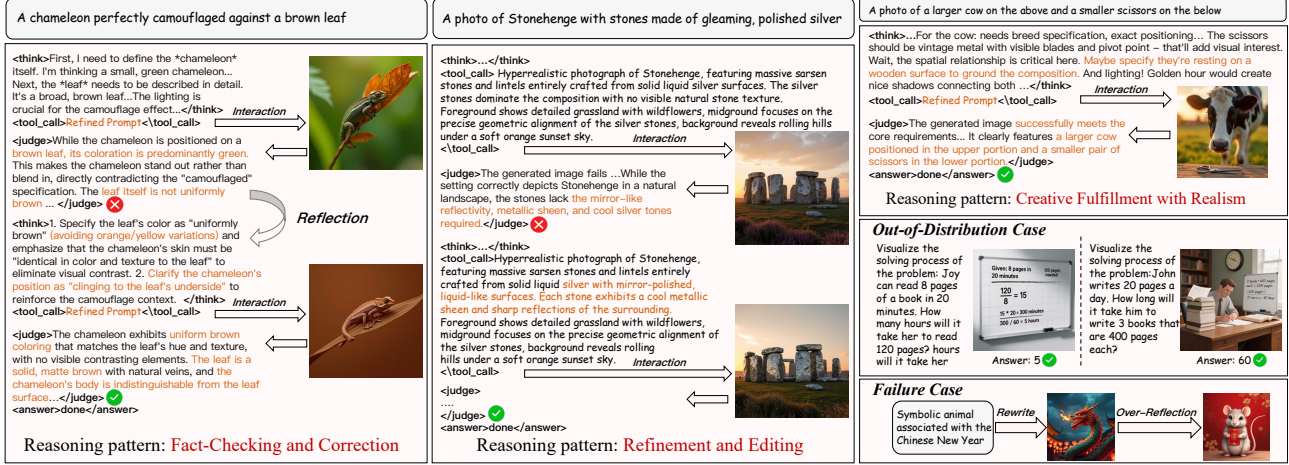


Figure 7. Case Studies of GenAgent. The figure illustrates three distinct reasoning patterns of GenAgent, its out-of-distribution generalization on a visual math task, and a representative failure case.

mizes prompts through introspective analysis. By the third interaction round (i.e., the second reflection), while the performance gains are more modest compared to the first round, further improvements remain achievable. Our analysis reveals that one contributing factor is the inherent capability ceiling of the underlying image generation model, which possesses intrinsic limitations in understanding complex semantics and fine-grained attributes that cannot be overcome through further prompt optimization. The experimental results indicate that two interaction rounds represent the optimal balance between performance and computational efficiency.

Training Dynamic. We further analyze model dynamics during RL training by tracking reward progression and the number of interaction rounds with the image generation tool, as illustrated in Figure 6. In the initial phase, the model exhibits a steady decrease in interactions with the image generation tool, suggesting that it first learns to leverage the rewriting capability rather than immediately engaging in multiple reflection rounds. This behavior corrects the over-reflection tendency inherited from the supervised fine-tuning phase. Subsequently, the model begins to increase interaction rounds to obtain pairwise rewards. As training progresses, both interaction rounds and rewards rise synchronously, demonstrating that the model has successfully learned when and how to perform effective reflection.

4.5. Case Study

Key Reasoning Patterns. We highlight three key reasoning patterns in GenAgent’s iterative process:

1) Fact-Checking and Correction: In the chameleon example (Figure 7, left), the agent detects a logical conflict—a green chameleon on brown leaves contradicts “perfectly camouflaged”—and revises the instruction to align color

and texture, demonstrating self-correction capability.

2) Refinement and Editing: For near-correct outputs like Stonehenge (Figure 7, mid), GenAgent performs targeted edits rather than full regeneration, adding specific descriptors (e.g., “mirror-polished”) to efficiently capture missing details like stone gloss.

3) Creative Fulfillment with Realism: The cow-and-scissors case (Figure 7, right-top) shows GenAgent balancing creativity with plausibility by constructing a convincing scene through composition, lighting, and perspective.

Out-of-Distribution Cases. Beyond these patterns, we test GenAgent on out-of-distribution tasks. Inspired by [26], we design a mathematical visualization task using GSM8K [5] problems (Figure 7, right-mid): GenAgent first reasons through the problem, then converts solution steps into detailed visual prompts, demonstrating strong potential for multimodal deep research.

Failure Case. We also identify a failure mode: Over-Reflection, where ambiguous prompts cause the agent to cycle through valid interpretations.

Further qualitative analyses, visual comparisons between different methods, and additional complete cases are provided in Supplementary Materials.

5. Conclusion

In this work, we explore how to construct agentic multimodal models that unify visual understanding and generation through active tool invocation. We introduce GenAgent, which decouples these capabilities—understanding is handled by the multimodal model itself, while generation leverages external models as tools. We conduct a two-stage training pipeline: SFT on high-quality tool invocation and reflection data, followed by reinforcement learning with pointwise and pairwise rewards to enable itera-

tive refinement. Our analysis reveals task-adaptive reasoning and cross-tool generalization, with reinforcement learning enabling complex multi-turn interactions. Extensive experiments demonstrate that our framework significantly enhances the generation performance of traditional diffusion models, achieving results comparable to powerful unified models, while maintaining greater flexibility and lower training costs. We hope our work offers an alternative perspective for advancing unified understanding and generation in multimodal models.

References

- [1] Shuai Bai, Keqin Chen, Xuejing Liu, Jialin Wang, Wenbin Ge, Sibo Song, Kai Dang, Peng Wang, Shijie Wang, Jun Tang, et al. Owen2. 5-vl technical report. *arXiv preprint arXiv:2502.13923*, 2025. [3](#), [5](#)
- [2] Juhai Chen, Zhiyang Xu, Xichen Pan, Yushi Hu, Can Qin, Tom Goldstein, Lifu Huang, Tianyi Zhou, Saining Xie, Silvio Savarese, et al. Blip3-o: A family of fully open unified multimodal models-architecture, training and dataset. *arXiv preprint arXiv:2505.09568*, 2025. [1](#), [2](#)
- [3] Juhai Chen, Le Xue, Zhiyang Xu, Xichen Pan, Shusheng Yang, Can Qin, An Yan, Honglu Zhou, Zeyuan Chen, Lifu Huang, et al. Blip3o-next: Next frontier of native image generation. *arXiv preprint arXiv:2510.15857*, 2025. [1](#)
- [4] Xiaokang Chen, Zhiyu Wu, Xingchao Liu, Zizheng Pan, Wen Liu, Zhenda Xie, Xingkai Yu, and Chong Ruan. Janus-pro: Unified multimodal understanding and generation with data and model scaling. *arXiv preprint arXiv:2501.17811*, 2025. [1](#), [2](#), [5](#)
- [5] Karl Cobbe, Vineet Kosaraju, Mohammad Bavarian, Mark Chen, Heewoo Jun, Lukasz Kaiser, Matthias Plappert, Jerry Tworek, Jacob Hilton, Reiichiro Nakano, et al. Training verifiers to solve math word problems. *arXiv preprint arXiv:2110.14168*, 2021. [8](#)
- [6] Gheorghe Comanici, Eric Bieber, Mike Schaeckermann, Ice Pasupat, Noveen Sachdeva, Inderjit Dhillon, Marcel Blisstein, Ori Ram, Dan Zhang, Evan Rosen, et al. Gemini 2.5: Pushing the frontier with advanced reasoning, multimodality, long context, and next generation agentic capabilities. *arXiv preprint arXiv:2507.06261*, 2025. [1](#), [4](#)
- [7] Chaorui Deng, Deyao Zhu, Kunchang Li, Chenhui Gou, Feng Li, Zeyu Wang, Shu Zhong, Weihao Yu, Xiaonan Nie, Ziang Song, et al. Emerging properties in unified multimodal pretraining. *arXiv preprint arXiv:2505.14683*, 2025. [1](#), [2](#), [5](#)
- [8] Chengqi Duan, Rongyao Fang, Yuqing Wang, Kun Wang, Linjiang Huang, Xingyu Zeng, Hongsheng Li, and Xihui Liu. Got-r1: Unleashing reasoning capability of mllm for visual generation with reinforcement learning. *arXiv preprint arXiv:2505.17022*, 2025. [2](#)
- [9] Robert Geirhos, Jörn-Henrik Jacobsen, Claudio Michaelis, Richard Zemel, Wieland Brendel, Matthias Bethge, and Felix A Wichmann. Shortcut learning in deep neural networks. *Nature Machine Intelligence*, 2020. [5](#)
- [10] Zigang Geng, Yibing Wang, Yeyao Ma, Chen Li, Yongming Rao, Shuyang Gu, Zhao Zhong, Qinglin Lu, Han Hu, Xisong Zhang, et al. X-omni: Reinforcement learning makes discrete autoregressive image generative models great again. *arXiv preprint arXiv:2507.22058*, 2025. [1](#), [2](#)
- [11] Dhruba Ghosh, Hannaneh Hajishirzi, and Ludwig Schmidt. Geneval: An object-focused framework for evaluating text-to-image alignment. *Advances in Neural Information Processing Systems*, 36:52132–52152, 2023. [5](#)
- [12] Melody Y Guan, Manas Joglekar, Eric Wallace, Saachi Jain, Boaz Barak, Alec Helyar, Rachel Dias, Andrea Vallone, Hongyu Ren, Jason Wei, et al. Deliberative alignment: Reasoning enables safer language models. *arXiv preprint arXiv:2412.16339*, 2024. [4](#)
- [13] Daya Guo, Dejian Yang, Haowei Zhang, Junxiao Song, Ruoyu Zhang, Runxin Xu, Qihao Zhu, Shirong Ma, Peiyi Wang, Xiao Bi, et al. Deepseek-r1: Incentivizing reasoning capability in llms via reinforcement learning. *arXiv preprint arXiv:2501.12948*, 2025. [4](#)
- [14] Jixiang Hong, Yiran Zhang, Guanzhong Wang, Yi Liu, Ji-Rong Wen, and Rui Yan. Reinforcing multimodal understanding and generation with dual self-rewards. *arXiv preprint arXiv:2506.07963*, 2025. [1](#), [2](#)
- [15] Dongzhi Jiang, Ziyu Guo, Renrui Zhang, Zhuofan Zong, Hao Li, Le Zhuo, Shilin Yan, Pheng-Ann Heng, and Hongsheng Li. T2i-r1: Reinforcing image generation with collaborative semantic-level and token-level cot. *NeurIPS*, 2025. [1](#), [2](#), [5](#)
- [16] Black Forest Labs. Flux. <https://github.com/black-forest-labs/flux>, 2024. [2](#), [4](#), [5](#)
- [17] Zijun Liu, Peiyi Wang, Runxin Xu, Shirong Ma, Chong Ruan, Peng Li, Yang Liu, and Yu Wu. Inference-time scaling for generalist reward modeling. *arXiv preprint arXiv:2504.02495*, 2025. [4](#)
- [18] Yuanhuiyi Lyu, Chi Kit Wong, Chenfei Liao, Lutao Jiang, Xu Zheng, Zexin Lu, Linfeng Zhang, and Xuming Hu. Understanding-in-generation: Reinforcing generative capability of unified model via infusing understanding into generation. *arXiv preprint arXiv:2509.18639*, 2025. [2](#)
- [19] Yuwei Niu, Munan Ning, Mengren Zheng, Weiyang Jin, Bin Lin, Peng Jin, Jiaqi Liao, Chaoran Feng, Kunpeng Ning, Bin Zhu, et al. Wise: A world knowledge-informed semantic evaluation for text-to-image generation. *arXiv preprint arXiv:2503.07265*, 2025. [1](#), [5](#)
- [20] OpenAI. Gpt-4o. <https://openai.com/index/introducing-4o-image-generation>, 2025. [1](#), [2](#), [5](#)
- [21] OpenAI. Thinking with images. <https://openai.com/index/thinking-with-images/>, 2025. [2](#)
- [22] QwenLM. Qwen3-vl. <https://github.com/QwenLM/Qwen3-VL>, 2025. [4](#), [5](#)
- [23] Ning Shang, Yifei Liu, Yi Zhu, Li Lyna Zhang, Weijiang Xu, Xinyu Guan, Buze Zhang, Bingcheng Dong, Xudong Zhou, Bowen Zhang, et al. rstar2-agent: Agentic reasoning technical report. *arXiv preprint arXiv:2508.20722*, 2025. [5](#)
- [24] Guangming Sheng, Chi Zhang, Zilingfeng Ye, Xibin Wu, Wang Zhang, Ru Zhang, Yanghua Peng, Haibin Lin, and Chuan Wu. Hybridflow: A flexible and efficient rlhf framework. *arXiv preprint arXiv: 2409.19256*, 2024. [5](#)

[25] Chengzhuo Tong, Ziyu Guo, Renrui Zhang, Wenyu Shan, Xinyu Wei, Zhenghao Xing, Hongsheng Li, and Pheng-Ann Heng. Delving into rl for image generation with cot: A study on dpo vs. grpo. *arXiv preprint arXiv:2505.17017*, 2025. 1, 2

[26] Jingqi Tong, Yurong Mou, Hangcheng Li, Mingzhe Li, Yongzhuo Yang, Ming Zhang, Qiguang Chen, Tianyi Liang, Xiaomeng Hu, Yining Zheng, et al. Thinking with video: Video generation as a promising multimodal reasoning paradigm. *arXiv preprint arXiv:2511.04570*, 2025. 8

[27] Team Wan, Ang Wang, Baole Ai, Bin Wen, Chaojie Mao, Chen-Wei Xie, Di Chen, Feiwu Yu, Haiming Zhao, Jianxiao Yang, et al. Wan: Open and advanced large-scale video generative models. *arXiv preprint arXiv:2503.20314*, 2025. 2

[28] Linqing Wang, Ximing Xing, Yiji Cheng, Zhiyuan Zhao, Donghao Li, Tiankai Hang, Jiale Tao, Qixun Wang, Rui-huang Li, Comi Chen, et al. Promptenhancer: A simple approach to enhance text-to-image models via chain-of-thought prompt rewriting. *arXiv preprint arXiv:2509.04545*, 2025. 1, 3, 5

[29] Zhenyu Wang, Aoxue Li, Zhenguo Li, and Xihui Liu. Genartist: Multimodal llm as an agent for unified image generation and editing. *Advances in Neural Information Processing Systems*, 37:128374–128395, 2024. 1, 2, 3

[30] Chengyue Wu, Xiaokang Chen, Zhiyu Wu, Yiyang Ma, Xingchao Liu, Zizheng Pan, Wen Liu, Zhenda Xie, Xingkai Yu, Chong Ruan, et al. Janus: Decoupling visual encoding for unified multimodal understanding and generation. In *Proceedings of the Computer Vision and Pattern Recognition Conference*, pages 12966–12977, 2025. 1, 2

[31] Chenfei Wu, Jiahao Li, Jingren Zhou, Junyang Lin, Kaiyuan Gao, Kun Yan, Sheng-ming Yin, Shuai Bai, Xiao Xu, Yilei Chen, et al. Qwen-image technical report. *arXiv preprint arXiv:2508.02324*, 2025. 1, 2, 5

[32] Mingrui Wu, Lu Wang, Pu Zhao, Fangkai Yang, Jianjin Zhang, Jianfeng Liu, Yuefeng Zhan, Weihao Han, Hao Sun, Jiayi Ji, et al. Reprompt: Reasoning-augmented reprompting for text-to-image generation via reinforcement learning. *arXiv preprint arXiv:2505.17540*, 2025. 1, 2, 3

[33] Enze Xie, Junsong Chen, Yuyang Zhao, Jincheng Yu, Ligeng Zhu, Chengyue Wu, Yujun Lin, Zhekai Zhang, Muyang Li, Junyu Chen, Han Cai, Bingchen Liu, Daquan Zhou, and Song Han. SANA 1.5: Efficient Scaling of Training-Time and Inference-Time Compute in Linear Diffusion Transformer, 2025. 7

[34] Jinheng Xie, Weijia Mao, Zechen Bai, David Junhao Zhang, Weihao Wang, Kevin Qinghong Lin, Yuchao Gu, Zhijie Chen, Zhenheng Yang, and Mike Zheng Shou. Show-o: One single transformer to unify multimodal understanding and generation. *arXiv preprint arXiv:2408.12528*, 2024. 2

[35] Junyan Ye, Dongzhi Jiang, Zihao Wang, Leqi Zhu, Zheng-hao Hu, Zilong Huang, Jun He, Zhiyuan Yan, Jinghua Yu, Hongsheng Li, et al. Echo-4o: Harnessing the power of gpt-4o synthetic images for improved image generation. *arXiv preprint arXiv:2508.09987*, 2025. 3, 5

[36] Qiyi Yu, Zheng Zhang, Ruofei Zhu, Yufeng Yuan, Xiaochen Zuo, Yu Yue, Weinan Dai, Tiantian Fan, Gao-hong Liu, Lingjun Liu, et al. Dapo: An open-source llm reinforcement learning system at scale. *arXiv preprint arXiv:2503.14476*, 2025. 4, 5

[37] Yi-Fan Zhang, Xingyu Lu, Shukang Yin, Chaoyou Fu, Wei Chen, Xiao Hu, Bin Wen, Kaiyu Jiang, Changyi Liu, Tianke Zhang, et al. Thyme: Think beyond images. *arXiv preprint arXiv:2508.11630*, 2025. 2

[38] Yaowei Zheng, Richong Zhang, Junhao Zhang, Yanhan Ye, Zheyuan Luo, Zhangchi Feng, and Yongqiang Ma. Llamafactory: Unified efficient fine-tuning of 100+ language models. In *Proceedings of the 62nd Annual Meeting of the Association for Computational Linguistics (Volume 3: System Demonstrations)*, Bangkok, Thailand, 2024. Association for Computational Linguistics. 5

[39] Yifan Zheng, Ziyu Wang, Ming Li, Jialiang Zhang, et al. Deepeyes: Towards agentic multimodal reasoning via tool-augmented vision models. *arXiv preprint arXiv:2501.01234*, 2025. 2, 4

[40] Le Zhuo, Liangbing Zhao, Sayak Paul, Yue Liao, Renrui Zhang, Yi Xin, Peng Gao, Mohamed Elhoseiny, and Hongsheng Li. From reflection to perfection: Scaling inference-time optimization for text-to-image diffusion models via reflection tuning. *ICCV*, 2025. 1, 2, 3, 5